LUPINE PUBLISHERS

Advances in Robotics & Mechanical Engineering

DOI: 10.32474/ARME.2022.03.000174

ISSN: 2643-6736

Review Article

Research on the Stiffness Performance of a Class of Limb for Parallel Robots as Machining Tools

Shuai Fan[1,2]*, Guanyu Shen[1], Tao Liu[1], Weibin Lan[2], Guangkui Song[3], Tao Ren1, Xu Luo[1]

[1]*School of mechanical and electrical Engineering, Chengdu University of Technology, People's Republic of China*

[2]*Center for Robotics, University of Electronic Science and Technology of China, Chengdu, People's Republic of China*

[3]*School of Mechanical and Electrical Engineering, University of Electronic Science and Technology of China, People's Republic of China*

***Corresponding author:** Shuai Fan, School of mechanical and electrical Engineering, Chengdu University of Technology, Chengdu, Sichuan, 610059, People's Republic of China

Received: August 18, 2022 **Published:** August 25, 2022

Abstract

Different from the previous conceptual design of configuration synthesis, the main purpose of the configuration synthesis used in the stiffness design is to compare the stiffness performance of different parallel robots. For a class of limbs used in the parallel robots as machining tools, the stiffness performances of different limbs are analyzed, and the comparison results between different limbs are given. The effects of different factors on the stiffness performance of different limbs are summarized, and some selection criteria of limbs are also presented. Thus, the stiffness performance of different parallel robots can be roughly judged in many configurations, which can provide a basis for selecting the configuration of the parallel robot.

Keywords: Parallel Robot; Configuration Synthesis; Stiffness Analysis; Machining Tool

Introduction

Owing to the structural advantages, parallel robots have been performed in low-speed and heavy-load tasks used in material processing of workpieces, such as the *Tricept TR600* launched by *Neos Robotics*, the *Hexapod* launched by *Ingersoll*, the *HP1* parallel robot launched by *Comau*, and the *IRB940* launched by *ABB*. After nearly 30 years of development, the research and application of some parallel robots as machine tools have achieved good results abroad. For example, *PKMtricept SL* company has developed a series of *Tricept-based* parallel robot, the *Exechon* parallel robot invented by *Neumann* has been applied to the milling of auto parts, the *Sprint Z3* power head has also been successfully used in the processing of aerospace components. Thanks to the efforts of many scholars, the theoretical research on parallel robots as machining tools has been presented such as the configuration synthesis, force/motion transfer characteristics, global stiffness performance, dynamic performance, vibration characteristics, kinematics calibration, error analysis, and others [1-6]. Nevertheless, the actual products of various novel parallel robots are rare, and even fewer have formed industrialized production. One of the important reasons is that there is a large deviation between the actual stiffness performance and the theoretical stiffness performance, which affects the machining accuracy of the parallel robots as machining tools (Figure 1) [7-12]. The stiffness performance of the parallel robot plays an important role in ensuring the machining accuracy, but the large difference between the theoretical design stiffness performance and the actual stiffness performance still often occurs, which seriously restricts the service of the parallel robot for high-precision machining scenarios. Generally, configuration synthesis, dimensional synthesis, and component synthesis are three approaches to optimize the stiffness performance of parallel robots. The main task of the configuration synthesis is to construct the specific structure of the robot according to the task requirements, where the number of limbs,

Copyright © All rights are reserved by Shuai Fan.

the distribution of limbs, the composition and order of the joints need to be determined. The configuration synthesis of parallel robots has developed rapidly at the end of the 20th century and the beginning of the 21st century. Many scholars have successively proposed many excellent configuration synthesis methods such as observation method, configuration evolution method, screw method, displacement subgroup theory method, GF set method. sports comprehensive method and others [13-16]. The previous research on configuration synthesis belongs to the category of early conceptual design, and its purpose is to use a certain method to discover a novel mechanism type or to include all configurations of parallel robots as much as possible. The use of these configuration synthesis methods has gradually matured, and the types of parallel robots included have the characteristics of a large number and variety (Table 1).

Table 1: A class of limb.

DOF	Joints	limbs	e.g.,	Stiffness
2	*R,P*	*RP,PR*	*PR*	2T/2R: $\Delta x, \Delta y, \Delta\varphi, \Delta\psi\left(\Delta z\right)$
3	*R,P,U*	*UP,PU*	*PU*	1T2R: $\Delta x, \Delta y, \Delta\psi\left(\Delta z\right)$
	RP	*RPR,RRP,PRR*		
4	*P,S*	*PS,SP*	*PS*	2T: $\Delta x, \Delta y, \left(\Delta z\right)$
	R,P,U	*RPU,RUP,PUR,PRU,UPR,URP*	*RPU*	1T1R: $\Delta x, \Delta\psi, \left(\Delta z\right)$
	R,P	*PRRR,RPRR,RRPR,RRRP*		
5	*P, U*	*UPU,PUU,UUP*	*UPU*	1T/1R: $\Delta x, \left(\Delta z\right) \big/ \Delta\psi, \left(\Delta z\right)$
	R,P,S	*RPS,RSP, PRS,PSR,SRP,SPR*	*RPS*	1T: $\Delta x, \left(\Delta z\right)$
6	*P,U,S*	*UPS,USP,PUS,PSU,SUP,SPU*	*UPS*	$\left(\Delta z\right)$
	P,S	*SPS,SSP,PSS,SSP*		
	R,P,U	*UPUR,UPRU,URPU*	*UPRU*	$\left(\Delta z\right)$

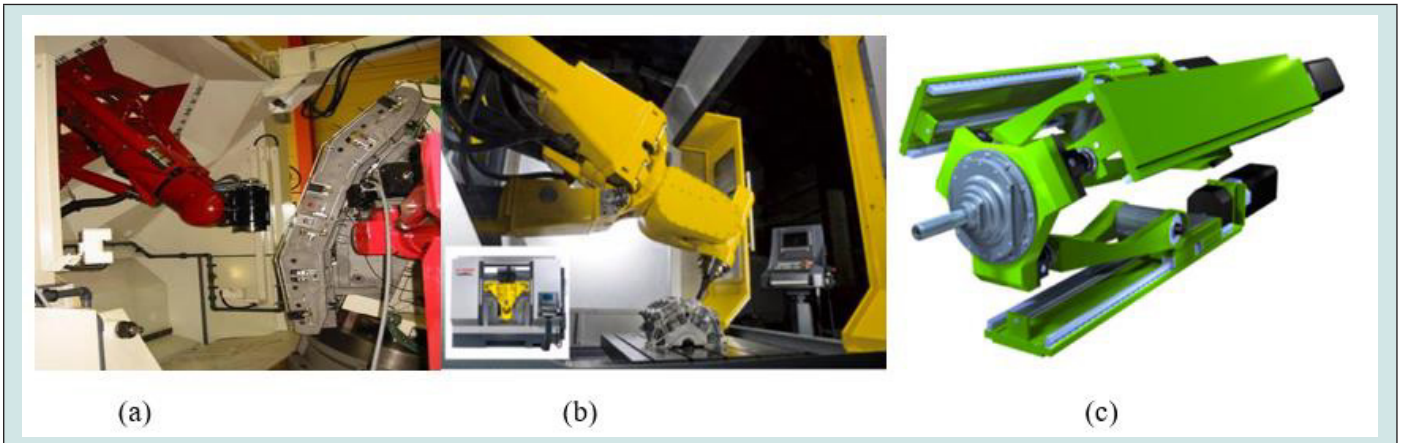

Figure 1: Parallel robots as parallel robots as machining tools: (a) Tricept, (b)Exechon, (c)Sprint Z3.

Different from the previous conceptual design of configuration synthesis, the main purpose of the configuration synthesis used in the stiffness design is to compare the stiffness performance of different parallel robots. However, if all the configurations are subjected to stiffness performance analysis and then the stiffness performance is compared, additional stiffness analysis will be introduced, which greatly increases the design workload. Through the research on the stiffness performance of the limb, the stiffness performance

of different parallel robots can be roughly judged in many configurations, which can provide a basis for selecting the configuration of the parallel robots. Selecting a class of limb of parallel robots as machining tools and analyzing the stiffness performance of each limb, the effects of different factors on the stiffness performance of different limbs can be summarized, and some selection criteria of limbs can be obtained. the results can greatly reduce the design workload and achieve the purpose of enhancement stiffness based on configuration synthesis. The remainder of this paper is organized as follows. In Section 2, stiffness analysis of a class of limb is presented. Then, in Section 3, stiffness comparisons of a class of limb are given. Finally, the study's conclusions are drawn (Table 2).

Table 2: Stiffness comparisons of a class of limb.

DOF		Δx	Δy	Δz	$\Delta\theta$	$\Delta\varphi$	$\Delta\psi$
2	*PR*	$2k^{cle}+2k^{con}+k^{def}$	$2k^{cle}+2k^{con}+k^{def}$	$0/\left(2k^{cle}+2k^{con}+k^{def}+k^{act}\right)$	0	$2k^{cle}+2k^{con}+k^{def}$	$2k^{cle}+2k^{con}+k^{def}$
3	*PU*	$3k^{cle}+3k^{con}+k^{def}$	$3k^{cle}+3k^{con}+k^{def}$	$0/\left(3k^{cle}+3k^{con}+k^{def}+k^{act}\right)$	0	0	$3k^{cle}+3k^{con}+k^{def}$
4	*PS*	$2k^{cle}+2k^{con}+k^{def}$	$2k^{cle}+2k^{con}+k^{def}$	$0/\left(2k^{cle}+2k^{con}+k^{def}+k^{act}\right)$	0	0	0
	RPU	$4k^{cle}+4k^{con}+k^{def}$	0	$0/\left(4k^{cle}+4k^{con}+k^{def}+k^{act}\right)$	0	0	$4k^{cle}+4k^{con}+k^{def}$
5	*UPU*	0	0	$0/\left(5k^{cle}+5k^{con}+k^{def}+k^{act}\right)$	0	0	$5k^{cle}+5k^{con}+k^{def}$
	RPS	$3k^{cle}+3k^{con}+k^{def}$	0	$0/\left(3k^{cle}+3k^{con}+k^{def}+k^{act}\right)$	0	0	$3k^{cle}+3k^{con}+k^{def}$
6	*UPS*	0	0	$0/\left(4k^{cle}+4k^{con}+k^{def}+k^{act}\right)$	0	0	0
	UPRU	0	0	$0/\left(6k^{cle}+6k^{con}+k^{def}+k^{act}\right)$	0	0	0

Stiffness Analysis of a Class of Limb

Under the background of applying parallel robots to machine tools, the stiffness characteristics of a common class of limb shown in Table 1 are studied [17-22]. A translation driving unit is considered in these limbs, and only four kinds of joints are considered including the rotation joint denoted by R, translation joint denoted by P, universal joint denoted by U and spherical joint denoted by S. If one end of the limb is fixed, the stiffness performance of each limb can be represented by the tiny deformation of the other end in six directions: $(\Delta x, \Delta y, \Delta z, \Delta\theta, \Delta\varphi, \Delta\psi)$. Obviously, there is zero deformation in the direction of the degrees of freedom, while there is deformation in the constraint directions [22].

Stiffness of Limbs With 2 DOFs

If the degree of freedom of the limb is 2, the limb that satisfies the above assumption information is composed of *PR* limb or *RP* limb. Taking the *PR* limb as an example, as shown in Figure 2, if the rotation axis of the rotation joint is along the direction of the x-axis and the moving axis of the translation joint is along the direction of the z-axis, the constraint direction of the limb to the end platform may include two pure forces along the direction of the x-axis and the direction of the y-axis and two couples around the direction of y-axis and the direction of z-axis. The stiffness characteristics in these four directions need to be considered. If the translation joint is the driving unit, the stiffness along the direction of z-axis should also be considered. Thus, the stiffness characteristics of the *PR* limb can be expressed as

$$\begin{cases} \Delta x = \Delta x_R^{cle} + \Delta x_P^{cle} + \Delta x_R^{con} + \Delta x_P^{con} + \Delta x_L^{def} \\ \Delta y = \Delta y_R^{cle} + \Delta y_P^{cle} + \Delta y_R^{con} + \Delta y_P^{con} + \Delta y_L^{def} \\ \Delta z = 0/\Delta z = \Delta z_R^{cle} + \Delta z_P^{cle} + \Delta z_R^{con} + \Delta z_P^{con} + \Delta z_L^{def} + \Delta z^{act} \\ \Delta\theta = 0 \\ \Delta\varphi = \Delta\varphi_R^{cle} + \Delta\varphi_P^{cle} + \Delta\varphi_R^{con} + \Delta\varphi_P^{con} + \Delta\varphi_L^{def} \\ \Delta\psi = \Delta\psi_R^{cle} + \Delta\psi_P^{cle} + \Delta\psi_R^{con} + \Delta\psi_P^{con} + \Delta\psi_L^{def} \end{cases} \quad (2\text{-}1)$$

where the superscript *cle* denote the clearances of each joint, the superscript def denote the deformation of links, and the superscript con denote the contact deformation of joints.

Stiffness of Limbs With 3 DOFs

If the degree of freedom of the limb is 3, the limb that satisfies the above assumption information is composed of *UP, PU, RPR, RRP* and *PRR*. Taking the *PU* limb as an example, as shown in Figure 2, if the rotation axis of the universal joint are along the direction of the x-axis and the direction of the y-axis and the moving axis of the

translation joint is along the direction of the z-axis, it can be seen that the constraint direction of the limb to the end platform may include two pure forces along the direction of the x-axis and the direction of the y-axis and one couples around the direction of z-axis. The stiffness characteristics in these three directions need to be considered. If the translation joint is the driving unit, the stiffness along the direction of z-axis should also be considered. Thus, the stiffness characteristics of the PU limb can be expressed as

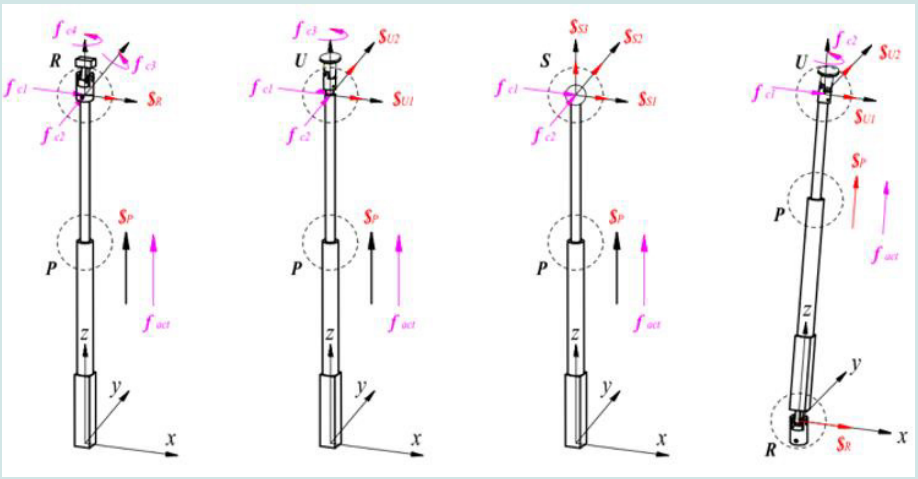

Figure 2: Schematic diagram of *PR, PU, PS* and *RPS* limbs.

$$\begin{cases} \Delta x = \Delta x_U^{cle} + \Delta x_P^{cle} + \Delta x_U^{con} + \Delta x_P^{con} + \Delta x_L^{def} \\ \Delta y = \Delta y_U^{cle} + \Delta y_P^{cle} + \Delta y_U^{con} + \Delta y_P^{con} + \Delta y_L^{def} \\ \Delta z = 0/\Delta z = \Delta z_U^{cle} + \Delta z_P^{cle} + \Delta z_U^{con} + \Delta z_P^{con} + \Delta z_L^{def} + \Delta z^{act} \\ \Delta \psi = \Delta \psi_U^{cle} + \Delta \psi_P^{cle} + \Delta \psi_U^{con} + \Delta \psi_P^{con} + \Delta \psi_L^{def} \\ \Delta \theta = \Delta \varphi = 0 \end{cases} \quad (2\text{-}2)$$

Stiffness of Limbs With 4 DOFs

If the degree of freedom of the limb is 4, the limb that satisfies the above assumption information is composed of *PS, SP, RPU, RUP, PUR, PRU, UPR, URP, PRRR, RPRR, RRPR* and *RRRP*. Taking the *PS* limb as an example, as shown in Figure 2, the possible constraint direction of the limb on the end platform may contain two pure forces along the direction of the x-axis and the direction of the y-axis. If the translation joint is the driving unit, the stiffness along the direction of z-axis should also be considered. Thus, the stiffness characteristics of the *PU* limb can be expressed as

$$\begin{cases} \Delta x = \Delta x_S^{cle} + \Delta x_P^{cle} + \Delta x_S^{con} + \Delta x_P^{con} + \Delta x_L^{def} \\ \Delta y = \Delta y_S^{cle} + \Delta y_P^{cle} + \Delta y_S^{con} + \Delta y_P^{con} + \Delta y_L^{def} \\ \Delta z = 0/\Delta z = \Delta z_S^{cle} + \Delta z_P^{cle} + \Delta z_S^{con} + \Delta z_P^{con} + \Delta z_L^{def} + \Delta z^{act} \\ \Delta \theta = \Delta \varphi = \Delta \psi = 0 \end{cases} \quad (2\text{-}3)$$

For the *RPU* limb, the constraint direction to the end platform may contain a pure force along the direction of x-axis and a couple around the direction of the z-axis. At this time, the stiffness characteristics of the *RPU* limb can be expressed as

$$\begin{cases} \Delta x = \Delta x_R^{cle} + \Delta x_P^{cle} + \Delta x_U^{cle} + \Delta x_R^{con} + \Delta x_P^{con} + \Delta x_U^{con} + \Delta x_L^{def} \\ \Delta z = 0/\Delta z = \Delta z_R^{cle} + \Delta z_P^{cle} + \Delta z_U^{cle} + \Delta z_R^{con} + \Delta z_P^{con} + \Delta z_U^{con} + \Delta z_L^{def} + \Delta z^{act} \\ \Delta \psi = \Delta \psi_R^{cle} + \Delta \psi_P^{cle} + \Delta \psi_U^{cle} + \Delta \psi_R^{con} + \Delta \psi_P^{con} + \Delta \psi_U^{con} + \Delta \psi_L^{def} \\ \Delta y = \Delta \theta = \Delta \varphi = 0 \end{cases} \quad (2\text{-}4)$$

Stiffness of Limbs With 5 DOFs

If the degree of freedom of the limb is 5, the limb that satisfies the above assumption information is composed of *UPU, PUU, UUP, RPS, RSP, PRS, PSR, SRP* and *SPR*. Taking the *UPU* limb as an example, as shown in Figure 3, the possible constraint direction of the limb on the end platform may contain one couple along the direction of the z-axis. If the translation joint is the driving unit, the stiffness along the direction of z-axis should also be considered. Thus, the stiffness characteristics of the *UPU* limb can be expressed as

$$\begin{cases} \Delta z = 0/\Delta z = \Delta z_{U1}^{cle} + \Delta z_P^{cle} + \Delta z_{U2}^{cle} + \Delta z_{U1}^{con} + \Delta z_P^{con} + \Delta z_{U2}^{con} + \Delta z_L^{def} + \Delta z^{act} \\ \Delta \psi = \Delta \psi_{U1}^{cle} + \Delta \psi_P^{cle} + \Delta \psi_{U2}^{cle} + \Delta \psi_{U1}^{con} + \Delta \psi_P^{con} + \Delta \psi_{U2}^{con} + \Delta \psi_L^{def} \\ \Delta x = \Delta y = \Delta \theta = \Delta \varphi = 0 \end{cases} \quad (2\text{-}5)$$

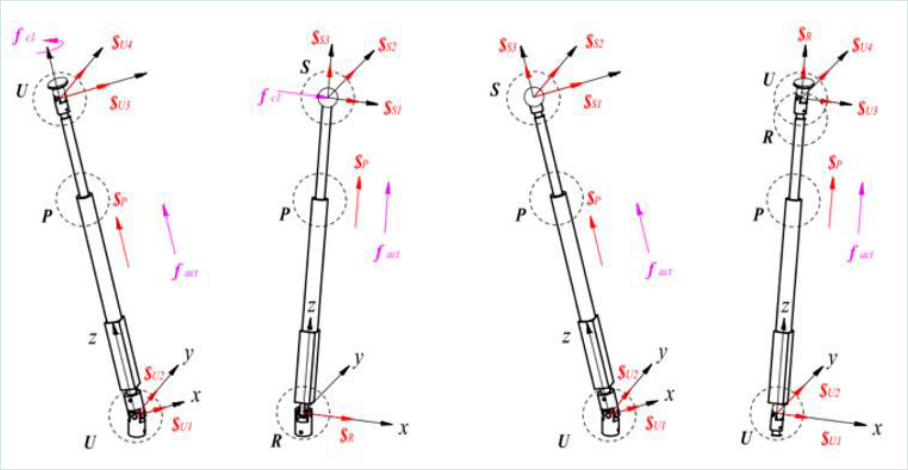

Figure 3: Schematic diagram of UPU, RPS, UPS and UPUR limbs.

For the *RPS* limb, the constraint direction to the end platform may contain a pure force along the direction of the x-axis that is the direction of the axis of the rotation joint. At this time, the stiffness characteristics of the *RPS* limb can be expressed as

$$\begin{cases} \Delta x = \Delta x = \Delta x_R^{cle} + \Delta x_P^{cle} + \Delta x_S^{cle} + \Delta x_R^{con} + \Delta x_P^{con} + \Delta x_S^{con} + \Delta x_L^{def} \\ \Delta z = 0/\Delta z = \Delta z_R^{cle} + \Delta z_P^{cle} + \Delta z_S^{cle} + \Delta z_R^{con} + \Delta z_P^{con} + \Delta z_S^{con} + \Delta z_L^{def} + \Delta z^{act} \\ \Delta y = \Delta\theta = \Delta\varphi = \Delta\psi = 0 \end{cases} \quad (2\text{-}6)$$

Stiffness of Limbs With 6 DOFs

If the degree of freedom of the limb is 6, the limb that satisfies the above assumption information is composed of *UPS, USP, PUS, PSU, SUP, SPU, SPS, SSP, PSS, SSP, UPUR, UPRU* and *URPU*. Taking the UPS limb as an example, as shown in Figure 3, the stiffness characteristics of the *UPS* limb can be expressed as

$$\begin{cases} \Delta x = \Delta y = \Delta\theta = \Delta\varphi = \Delta\psi = 0 \\ \Delta z = 0/\Delta z = \Delta z_U^{cle} + \Delta z_P^{cle} + \Delta z_S^{cle} + \Delta z_U^{con} + \Delta z_P^{con} + \Delta z_S^{con} + \Delta z_L^{def} + \Delta z^{act} \end{cases} \quad (2\text{-}7)$$

For the *UPRU* limb, the limb has no constraint on the end platform, and the stiffness characteristics of the *UPRU* limb can be expressed as

$$\begin{cases} \Delta x = \Delta y = \Delta\theta = \Delta\varphi = \Delta\psi = 0 \\ \Delta z = 0/\Delta z = \Delta z_{S1}^{cle} + \Delta z_P^{cle} + \Delta z_{S2}^{cle} + \Delta z_{S1}^{con} + \Delta z_P^{con} + \Delta z_{S2}^{con} + \Delta z_L^{def} + \Delta z^{act} \end{cases} \quad (2\text{-}8)$$

Stiffness Comparisons of a Class of Limb

For the parallel robot with few degrees of freedom, the stiffness performance of the driving directly affects the stiffness performance in the directions of the degree of freedom of the parallel robot, and the stiffness performance in the constraint direction at the end of the limb directly affects the stiffness performance in the constraint directions of the parallel robot. If the gap between two components of a joint is equal to k^{cle}, the contact deformation between two components of a joint is k^{con}, the link deformation is k^{def}, and the driving stiffness is k^{act}, the stiffness characteristics of the above-mentioned limbs are listed in Table 2, where the effects of component information and scale information are ignored. Obviously, the stiffness performance relationship of the eight limbs in the direction of freedom is:

$$PR = PS > PU = RPS > RPU = UPS > UPU > UPRU \quad (3\text{-}1)$$

The stiffness performance of the limb cannot be reveled directly by the degree of freedom of the limb. At the same time, the less the number of joints, the better the stiffness performance of the limb. The reason is that when the number of joints is large, the more active components are introduced, which will increase the effects of joint gap, contact deformation, and rod deformation. In addition, comparing the *UPS* limb and *UPRU* limb, the use of composite joints will increase the size of the limb gap and reduce the stiffness performance of the limb.

Conclusions

In the configuration synthesis, the main factors affecting the stiffness performance of the parallel robot include the type of limb, the distribution of joints in the limb, and the number of limbs. The stiffness enhancement method of parallel robot can be approached by adding the number of limbs, improving the distribution of joints, and changing the type of limbs. The stiffness performance criterion in configuration synthesis can be summarized as follows:

a. The degree of freedom of the limb cannot directly affect the stiffness performance of the limb.

b. The smaller number of active joints, the smaller deformation of the limb.

c. The smaller number of joints, the smaller joint gap of limbs. The use of composite joints will increase the size of the joint gap of limbs, which will reduce the stiffness performance of the limb.

d. The greater number of limbs, the better stiffness performance of parallel robots. The uniform distribution of the limbs on the

fixed platform, and the mobile platform can also make the stiffness performance more uniform.

e. The effect of the distribution of joints on the stiffness performance of the limb is uncertain. The change of the joint order of some limbs has no effect on the stiffness of the limb, and the change of the joint order of some limbs will increase the stiffness of the limb.

Competing interests

The authors declare no competing financial interests.

Funding

This work was supported by the National Natural Science Foundation of China [grant numbers: 51875086]and the Sichuan Science and Technology Program [2021YFS0305].

Acknowledgement

Not applicable.

Acknowledgements

Sponsorship of this research by the National Natural science foundation of China under grant no. 51271125 is gratefully acknowledged.

References

1. LP Wang, BB Zhang, J Wu (2016) Optimum design of a 4-PSS-PU redundant parallel manipulator based on kinematics and dynamics[J]. Proceedings of the Institution of Mechanical Engineers Part C-Journal of Mechanical Engineering Science 230(13): 2273-2284.
2. S Fan, SW Fan, WB Lan (2020) A new approach to enhance the stiffness of heavy-load parallel robots by means of the component selection[J]. Robotics and Computer Integrated Manufacturing 61: 1-18.
3. GL Wu, B Niu (2018) Dynamic stability of a tripod parallel robotic wrist featuring continuous end-effector rotation used for drill point grinder[J]. Mechanism and Machine Theory 129: 36-50.
4. ZL Zhou, J Xi, CK Mechefske (2006) Modeling of a fully flexible 3PRS manipulator for vibration analysis. J Mech Des 128: 403-412.
5. ZH Xie, FG Xie, XJ Liu, JS Wang (2021) Global G (2003) continuity toolpath smoothing for a 5-DoF machining robot with parallel kinematics [J]. Robotics and Computer-Integrated Manufacturing 67: 1-11.
6. D Wang, LP Wang, J Wu (2021) Physics-based mechatronics modeling and application of an industrial-grade parallel tool head[J]. Mechanical System and Signal Processing 148: 1-7.
7. CL Dong, HT Liu, W Yue, T Huang (2018) Stiffness modeling and analysis of a novel 5-DOF hybrid robot[J]. Mechanism and Machine Theory 125: 80-93.
8. T Sun, BB Lian (2018) Stiffness and mass optimization of parallel kinematic machine[J]. Mechanism and Machine Theory 120: 73-88.
9. CL Dong, HT Liu, JL Xiao, T Huang (2021) Dynamic modeling and design of a 5-DOF hybrid robot for machining[J]. Mechanism and Machine Theory 165: 104438.
10. A Joubair, M Slamani, IA Bonev (2012) Kinematic calibration of a 3-DOF planar parallel robot[J]. Industrial Robot-an International Journal 39(4): 392-400.
11. X Kong, CM Gosselin (2004) Type synthesis of 3-DOF translational parallel manipulators based on screw theory[J]. Journal of Mechanical Design 126(1): 83-92.
12. Z Huang, QC Li (2003) Type synthesis of symmetrical lower-mobility parallel mechanisms using the constraint-synthesis method[J]. International Journal of Robotics Research 22(1): 59-79.
13. JM Herve (1999) The Lie group of rigid body displacements, a fundamental tool for mechanism design[J]. Mechanism and Machine Theory 34(5): 719-730.
14. A Pashkevich, D Chablat, P Wenger (2009) Stiffness analysis of over constrained parallel manipulators[J]. Mechanism and Machine Theory 44(5): 966-982.
15. B Hu, Y Lu (2011) Solving stiffness and deformation of a 3-UPU parallel manipulator with one translation and two rotations[J]. Robotica 29(6): 815-822.
16. M Gallant, C Gosselin (2018) Singularities of a planar 3-RPR parallel manipulator with joint clearance[J]. Robotica 36(7): 1098-1109.
17. XC Zhang, XM Zhang, Z Cheng (2014) Dynamic analysis of a 3-RRR parallel mechanism with multiple clearance joints[J]. Mechanism and Machine Theory 78: 105-115.
18. GX Wang (2019) Dynamics analysis of parallel mechanism with flexible moving platform based on floating frame of reference formulation[J]. Journal of Mechanism and Robotics-Transactions of the ASME 11(4): 1-11.
19. J Jiao, Y Wu, KP Yu, R Zhao (2019) Dynamic modeling and experimental analyses of Stewart platform with flexible hinges[J]. Journal of vibration and Control 25(1): 151-171.
20. M Hafezipour, S Khodaygan (2017) An uncertainty analysis method for error reduction in end-effector of spatial robots with joint clearances and link dimension deviations[J]. International Journal of Computer Integrated Manufacturing 30(6): 653-663.
21. Y Qi, T Sun, YM Song (2018) Multi-objective optimization of parallel tracking mechanism considering parameter uncertainty[J]. Journal of Mechanism and Robotics-Transactions of the ASME 10(4): 1-12.
22. WA Cao, HF Ding, WG Zhu (2019) Stiffness modeling of over constrained parallel mechanisms under considering gravity and external payloads[J]. Mechanism and Machine Theory 135: 1-16.
23. X Chen, XJ Liu, FG Xie, T Sun (2014) A comparison study on motion/force transmissibility of two typical 3-DOF parallel manipulators: the sprint Z3 and A3 tool heads[J]. International Journal of Advanced Robotic Systems 11(1): 1-5.
24. S Fan, SW Fan (2019) Approximate Stiffness Modelling and Stiffness Defect Identification for a Heavy-load Parallel Manipulator. Robotica 37: 1120-1142.

This work is licensed under Creative Commons Attribution 4.0 License

To Submit Your Article Click Here: Submit Article

DOI: 10.32474/ARME.2022.03.000173

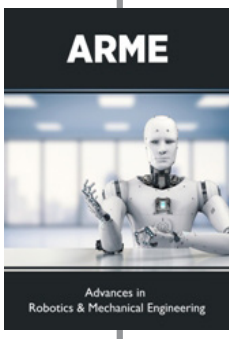

Advances in Robotics & Mechanical Engineering

Assets of Publishing with us

- Global archiving of articles
- Immediate, unrestricted online access
- Rigorous Peer Review Process
- Authors Retain Copyrights
- Unique DOI for all articles